Hindawi
Wireless Communications and Mobile Computing
Volume 2022, Article ID 2986536, 17 pages
https://doi.org/10.1155/2022/2986536

Research Article

Design and Analysis of a Compact Superwideband Millimeter Wave Textile Antenna for Body Area Network

Mohammad Monirujjaman Khan,[1] **Kaisarul Islam**,[1] **Md. Nakib Alam Shovon**,[1] **Muhammad Inam Abbasi**,[2] **Sami Bourouis**,[3] **Hany S. Hussein**,[4,5] **and Hammam Alshazly**[6]

[1]*Department of Electrical and Computer Engineering, North South University, Dhaka-1229, Bangladesh*
[2]*Centre for Telecommunication Research & Innovation (CETRI), Faculty of Electrical and Electronic Engineering Technology (FTKEE), Universiti Teknikal Malaysia Melaka (UTeM), Melaka 76100, Malaysia*
[3]*Department of Information Technology, College of Computers and Information Technology, Taif University, P.O. Box 11099, Taif 21944, Saudi Arabia*
[4]*Electrical Engineering Department, Faculty of Engineering, King Khalid University, Abha 62529, Saudi Arabia*
[5]*Electrical Engineering Department, Faculty of Engineering, Aswan University, Aswan 81528, Egypt*
[6]*Faculty of Computers and Information, South Valley University, Qena 83523, Egypt*

Correspondence should be addressed to Mohammad Monirujjaman Khan; monirujjaman.khan@northsouth.edu and Kaisarul Islam; islam.kaisarul@northsouth.edu

Received 1 November 2021; Revised 26 January 2022; Accepted 18 February 2022; Published 18 March 2022

Academic Editor: Issa Elfergani

The advancement of wireless technology has led to an exponential increase in the usage of smart wearable devices. Current wireless bands are getting more congested, and we are already seeing a shift towards millimeter wave bands. This paper proposes a design for a millimeter wave textile antenna for body-centric communications. The antenna has a quasi-self-complementary (QSC) structure. The radiating patch is a semicircular disc with a radius of 1.855 mm and is fed by a 5.07 mm long, 0.70 mm wide microstrip feedline. A complementary leaf-shaped slot is etched in the ground plane. The radiating disc and the ground plane are attached to a 1.5 mm thick nonconducting 100% polyester substrate. The antenna has an overall dimension of 10 mm × 7.00 mm. In free space, the antenna achieved a superwideband impedance bandwidth that covers the K_a, V, and W bands designated by IEEE. At 60 GHz, the antenna's radiation efficiency was 89.06%, with a maximum gain of 5.7 dBi. Millimeter waves are easily blocked by obstacles and have low skin penetration depth. On-body investigations were carried out by placing the antenna on a human phantom at five different distances. No significant amount of back radiation was observed. The radiation efficiency decreased to 67.48% at 2 mm away from the phantom, while the maximum gain slightly increased. The efficiency and radiation patterns improved as the distance between the antenna and the phantom gradually increased. Ten different textile substrates were also used to test the antenna. With a few exceptions, the free space and on-body simulation results were very similar to polyester. The design and simulation of the antenna were carried out using the CST microwave studio.

1. Introduction

Wearable technology has grown rapidly in the last decade, simultaneously increasing the popularity of devices like fitness trackers and smart watches. These devices are used to collect health monitoring data and communicate with other devices, like a smartphone. Due to the high demand for connectivity, current wireless bands are getting more congested, and as a result, millimeter wave (mmWave) bands are generating more interest for future communication. The

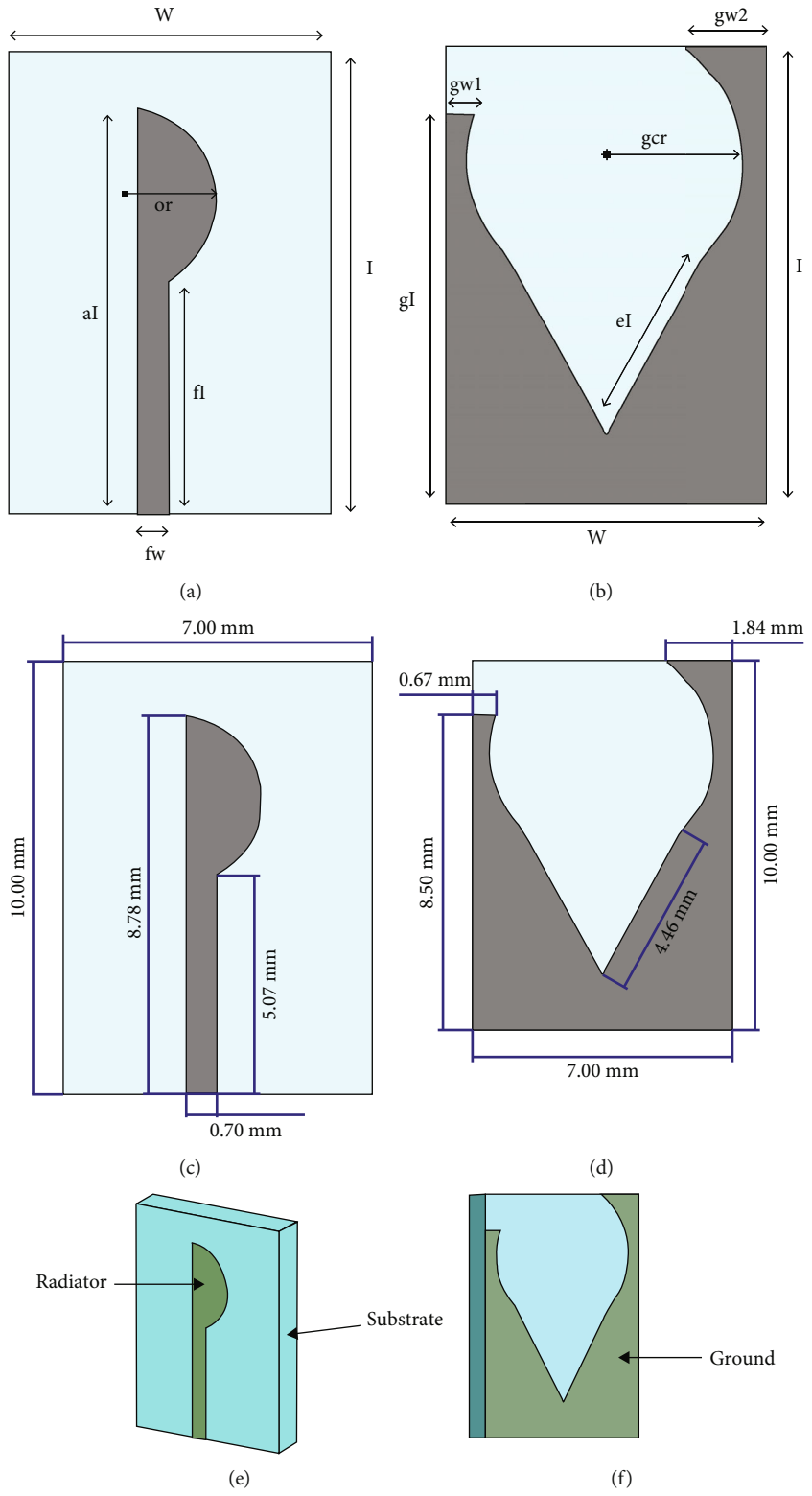

Figure 1: Continued.

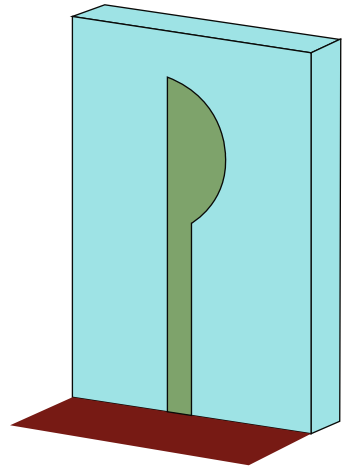

(g)

Figure 1: Parameters of the proposed antenna: (a) front view, (b) bottom view, (c) front view with dimension, (d) back view with dimension, (e) perspective front view, (f) perspective back view, and (g) antenna with a waveguide port.

Table 1: Values for antenna dimensions.

S. no.	Parameter	Value (mm)
1	w	7
2	l	10
3	or	2
4	wcr	3
5	gw1	0.67
6	gl	8.5
7	fw	0.7
8	fl	5.07
9	al	8.78
10	gw2	1.84
11	el	4.46

millimeter wave offers communication bands with an enormous amount of bandwidth, with data rates reaching up to 10 Gbps. mmWave occupies from 30 GHz to 300 GHz, which means the wavelength is very short over the whole spectrum. The shorter size of the wavelength makes mmWave highly susceptible to physical obstacles and requires line-of-sight (LOS) communication. Signals get easily attenuated due to high atmospheric absorption, effectively reducing the transmission range. Millimeter wave beams are very narrow, and due to short-range property, they are less vulnerable to interference and therefore provide high security [1]. At present, mmWave technology is being used in many applications like satellite communications, automotive navigation, 5G networks, medical fields, and many more areas [2, 3].

Traditional electronic circuits and antennas are made from rigid materials. It is desirable for wearable devices to have good flexibility. Textile antennas are a convenient technology that shows great potential in its ability to integrate directly into garments, thus providing great flexibility. There are two main types of textile antennas—conducting textile antennas and nonconducting textile antennas [4]. Conducting textiles, also known as electrotextiles, are made from metal-coated conductive threads or by coating a metal layer on a normal fabric [5]. On the other hand, nonconducting textile antennas use the fabric itself as the substrate layer of the antenna. An antenna's performance is dependent on the dielectric permittivity of the fabric.

A body-centric wireless network (BCWN) is a network of nodes working close to the human body. When these nodes are placed outside but close to a human body, the mode of operation is called "on-body." As a result of the human body acting as a lossy medium, on-body antennas, particularly textile antennas, are prone to performance degradation. Textile antennas are sensitive to wet, wrinkling, and bending circumstances in addition to the lossy medium. It is therefore necessary to evaluate textile antennas for on-body applications. In this paper, we are proposing the design of a nonconducting quasi-self-complementary textile antenna based on a 100% polyester substrate. The antenna will have a superwideband that will cover the K_a (27 to 40 GHz), V (40 to 75 GHz), and W (75 to 110 GHz) bands designated by IEEE. For on-body communications, the antenna will also be analyzed by keeping it at certain distances from a human body phantom. The antenna will also be evaluated by ten different textile materials. The design and simulation process will be carried out with Computer Simulation Technology (CST) Microwave Studio.

In 2001, the 60 GHz band (57-64 GHz) was released by the Federal Communications Commission (FCC) for unlicensed use. This has garnered much research interest producing various types of 60 GHz antenna designs. Impedance bandwidth ranging from 4 to 10 GHz with high gain has been investigated for on-body applications in [6–12]. There are very few textile antenna designs proposed for the mmWave spectrum. Two antenna designs—a Yagi-Uda and a four-patch array based on a 0.2 mm thick cotton substrate—are proposed in [13, 14], respectively. At the mmWave spectrum, it is difficult to manufacture

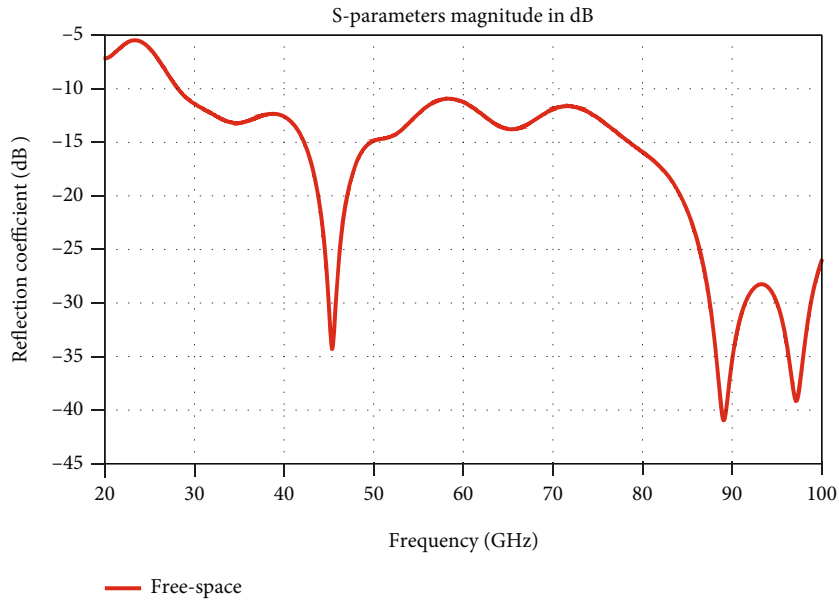

Figure 2: The proposed design's simulated free space return loss.

electrotextiles due to the inaccurate cutting process. For this reason, a thin copper foil with a thickness of 0.07 mm has been used as the conducting material for both designs. A driven dipole with ten directors printed on the textile makes up the Yagi-Uda antenna. In both free space and on-body situations, the return loss curve demonstrates that the antenna is well matched from 57 to 64 GHz. The antenna is 48% efficient with a maximum gain of 11.9 dBi. The four-patch array antenna is printed with a 15.2 mm long microstrip feedline on the cotton substrate. The measured reflection coefficient shows good impedance bandwidth in the 57-64 GHz range. Under crumpling conditions, the antenna's gain is dropped by 1 dB, but the reflection coefficient is largely unaffected for body-centric communication.

A circularly polarized dielectric resonator antenna (DRA) was presented in [15] for off-body communications. This antenna was designed on an ECCOSTOCK HiK substrate with a dielectric value of 10. At -10 dB impedance, the antenna operates in the frequency range of 6.95–8.68 GHz with good performance. A multiple-input multiple-output (MIMO) DRA antenna for WiMax application is proposed in [16]. The antenna is wideband and circularly polarized. A DRA antenna has been proposed for 5G New Radio (5G NR) applications [17]. The antenna is intended to be used in the sub-6 GHz spectrum. Employing wireless signals, a deep learning approach for subject-independent emotion recognition has been developed in [18]. In WBANs, [19] proposed a machine learning approach for detecting sensor data modification intrusions.

The majority of polyester-based textile antennas are intended for use in the ultra-wideband spectrum [19–24]. In [25], the authors propose a polyester-based textile antenna for use in a 5G cellular network running at the 26 GHz range. The antenna structure contains an electromagnetic bandgap (EBG) structure to enhance the antenna's performance. With a maximum gain of 8.65 dBi, the measured bandwidth was 0.91 GHz. A patch antenna for wireless communications was presented in [26]. The antenna was fed by a microstrip path, and it works at 60 GHz with wide bandwidth. The antenna was not tested for body-centric communications (BCWCc). In [27], an mmWave Q-Slot antenna for BCWCs was presented. The antenna was printed on the FR-4 substrate. The antenna's overall width and length were 12.9 mm and 14 mm, respectively. From our literature review, we could not find any polyester substrate antenna that covers the entire K_a, V, and W bands. The design and study of a compact superwideband millimeter wave textile antenna for body area networks are the paper's main contribution. The antenna is printed on a non-conducting 100% polyester substrate. The antenna is superwideband, and, at a -10 dB return loss, this antenna works in the frequency range of 28 GHz to 100 GHz. After initial design, the antenna was designed on different substrates to investigate the performance. Using CST software, the antenna was modelled in free space as well as on a three-layer human phantom. The results are compared in both open space and on the body. The novelty of this antenna is that it has a very large bandwidth and it is very compact in size as well, compared to the available antennas reported in the literature. The antenna has been designed on a 100% polyester substrate, which is a new design for a 60 GHz mm-wave antenna in BAN application. This work will be the first to present a polyester-based mmWave antenna that covers a superwide bandwidth.

The paper is divided into six sections, which includes the Introduction and the Conclusion. Antenna design details are discussed in Section 2. Section 3 contains the results of the free space simulation. In Section 4, on-body results are included. Free space and on-body simulation results of various textile materials are discussed in Section 5.

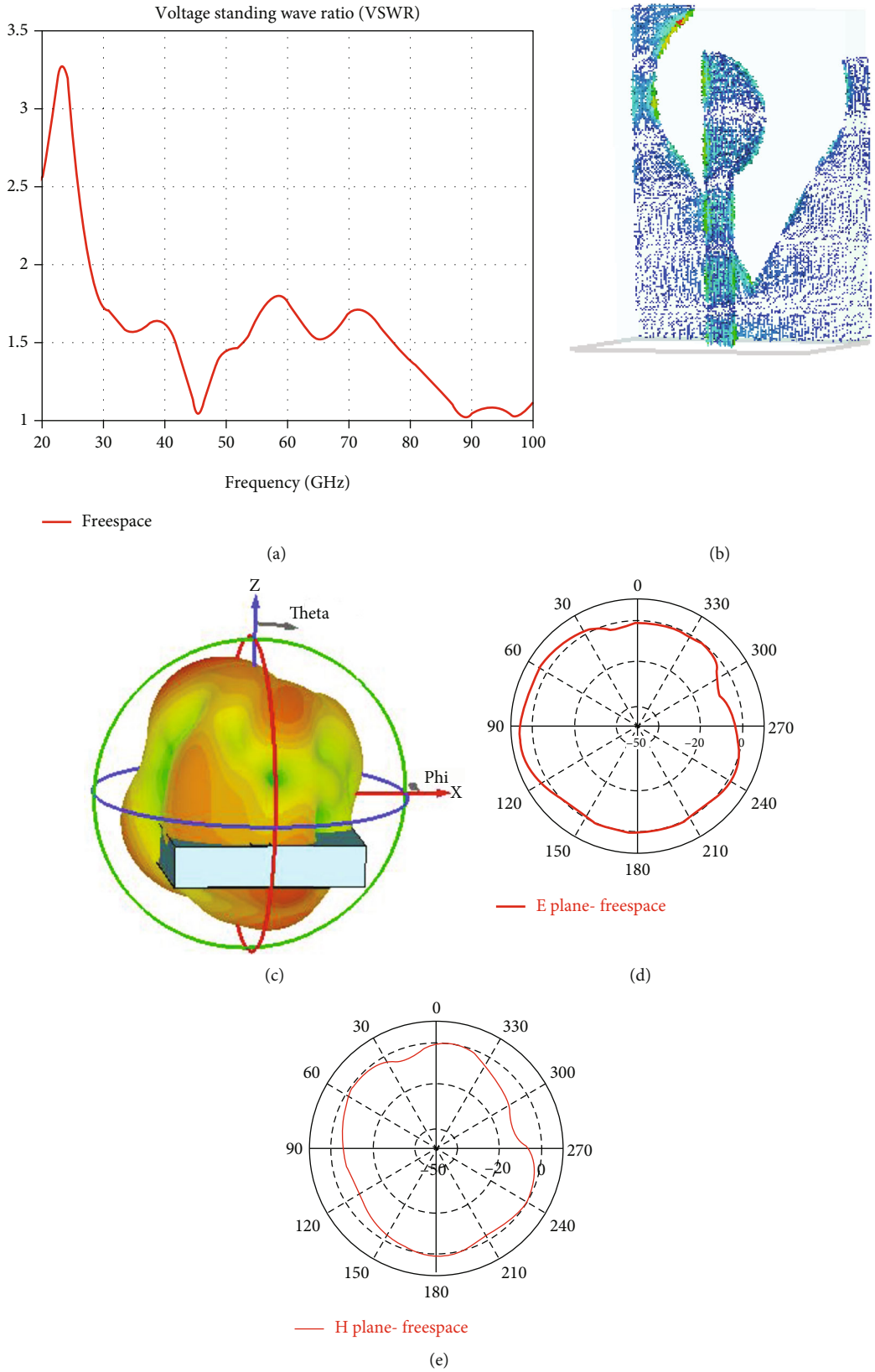

Figure 3: (a) VSWR, (b) surface current at 60 GHz, (c) 3D radiation pattern, (d) E plane radiation pattern at 60 GHz, and (e) H plane radiation pattern at 60 GHz.

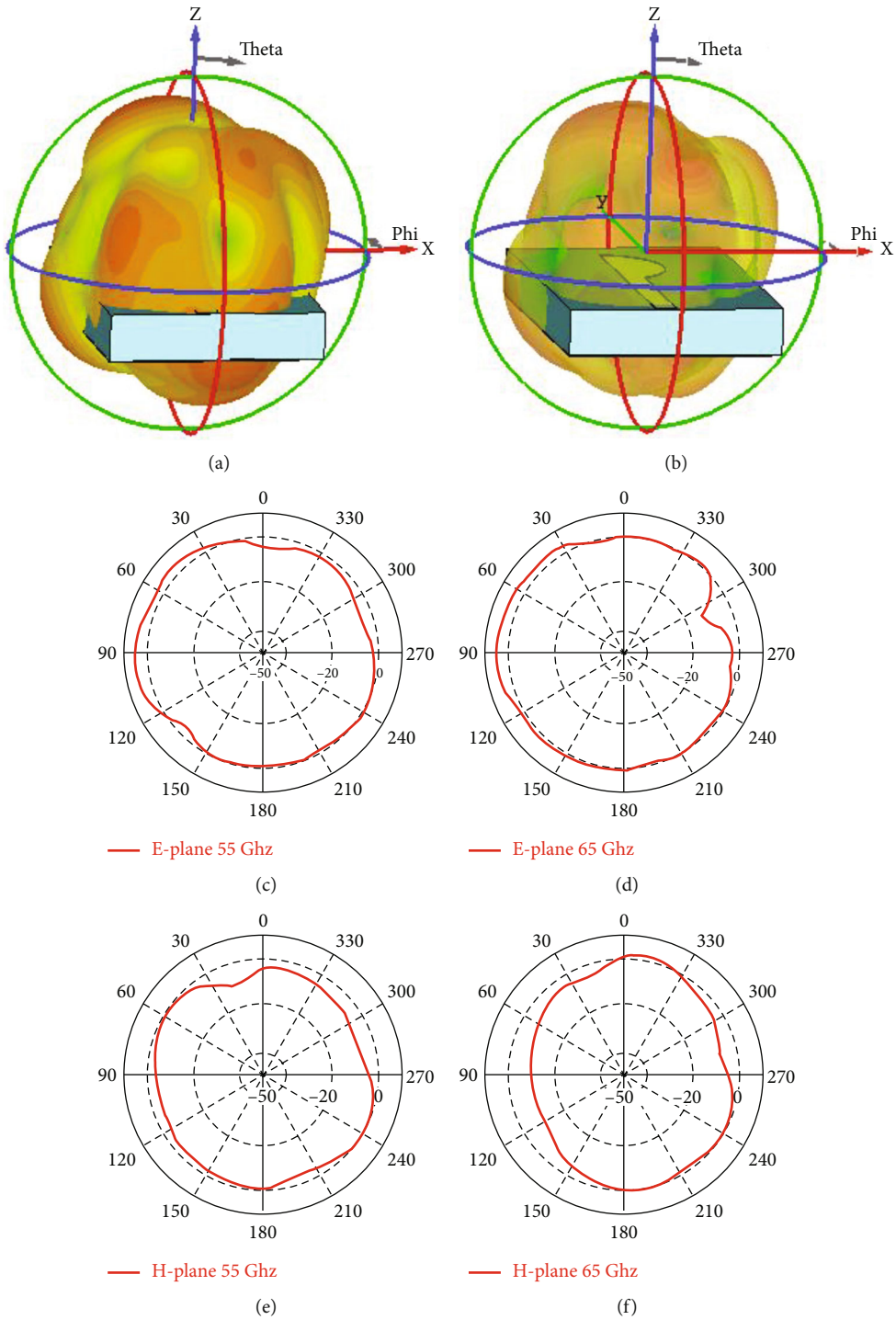

Figure 4: (a) 3D radiation at 55 GHz, (b) 3D radiation at 65 GHz, (c) E plane radiation at 55 GHz, (d) E plane radiation at 65 GHz, (e) H plane radiation at 55 GHz, and (f) H plane radiation at 65 GHz.

2. Antenna Design

Figures 1(a)–1(g) show the details of the antenna design. Three layers make up the quasi-self-complementary antenna. The antenna is designed on a 10 mm × 7.00 mm, 1.5 mm thick 100% polyester substrate. The relative permittivity (ε_r) of polyester is 1.9. In this research, the loss tangent of the polyester substrate has been considered 0.0045. The radiating patch is a semicircular disc with a radius of 1.855 mm placed on top of the substrate. The apex of the disc is 2 mm away from a point on the substrate, and this distance is denoted by "or" in Figure 1. The ground plane is etched with a leaf-shaped slot that complements the radiating patch and is linked to the substrate's bottom layer.

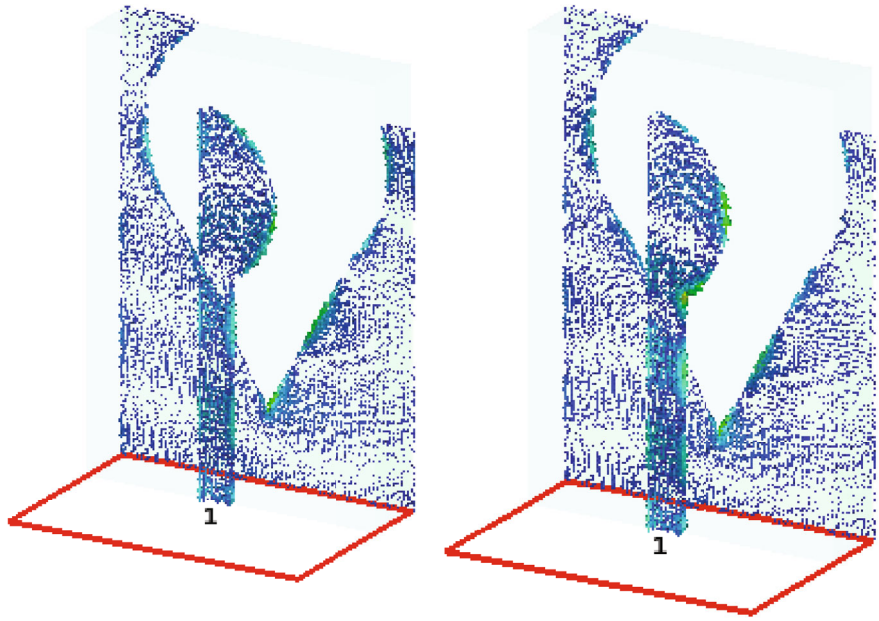

(a) (b)

Figure 5: (a) Current distribution at 55 GHz and (b) current distribution at 65 GHz.

Perfect Electric Conductor (PEC) material has been used as a patch and ground. The thickness of the ground plane and path is 0.035 mm.

The leaf shape is etched from three distinct coexisting slots—a circular, a rectangular, and a triangular slot. The circular slot has a radius of 3 mm (denoted by "gcr" in Figure 1). A small rectangular slot, measuring 1.5 mm × 0.67 mm, is etched from the right-top corner of the ground. The width of this slot is denoted by "gw1" in Figure 1. This rectangular slot creates a partial side ("gl") on the ground and is on the same side as the semicircular disc is facing. Lastly, an isosceles triangular slot completes the overall shape of the ground slot. The triangle's legs are denoted by "el" in Figure 1 and measure 4.46 mm. A microstrip feedline with a length of 5.07 mm and a width of 0.70 mm feeds the antenna. The dimension of each of these parameters are given in Table 1. The radiating patch, feedline, and ground are made from 0.035 mm thick Perfect Electric Conductor (PEC).

3. Free Space Simulation Results

In free space, the antenna's return loss curve shows a super-wide impedance bandwidth of more than 78 GHz. From Figure 2, it is noted that the antenna works very well at -10 dB impedance from 28 GHz to 100 GHz. The impedance bandwidth of this antenna is very large. Three different resonant frequencies were observed—one in the V band and two others in the W band region (Figure 2). The voltage standing wave ratio (VSWR) at these frequencies is very close to the desired value of 1 (Figure 3(a)). At 60 GHz, a good radiation pattern was observed in the E plane (Figure 3(d)), while the H plane (Figure 3(e)) had very limited radiation with a narrow beam width. The return loss magnitude at this frequency is -11.25 dB. The maximum gain is 5.7 dBi with a radiation efficiency of 89.06%. The majority of the surface current is concentrated along the semicircular disc's straight edges and the ground's equivalent inner side edges (Figure 3(b)). At 60 GHz, the 3D radiation pattern is seen in Figure 3(c). The 3D radiation looks like the antenna radiates towards the Z direction with some distortion at different angles.

Figures 4(a) and 4(b) depict the antenna's 3D radiation pattern at 55 and 65 GHz, respectively. At 55 GHz and 65 GHz, the E and H plane radiation patterns are shown in Figures 4(c)–4(f). In this study, it is observed that at lower and higher frequencies of 55 GHz and 65 GHz, the radiation patterns are nearly comparable. At 65 GHz, the radiation patterns in both planes are slightly distorted at certain angles. Figures 5(a) and 5(b) show the current distribution of the antenna at 55 GHz and 65 GHz.

The return loss curve was barely affected by a change in the dimension of the feed width (fw), while other parameters of the antenna were kept constant (Figure 6(a)). The ground plane's circular slot size is denoted by the radius "gcr." The optimum radius size is 3 mm. Decreasing the radius to 2.9 mm and 2.8 mm had an insignificant effect on the impedance bandwidth (Figure 6(b)). The relative position of the radiating semicircular disc with respect to a fixed point on the substrate is denoted by the word "or." The optimum value of "or" is 2 mm. When the radiating disc is closer to the point; i.e., the position of the disc is moved slightly to the left, the return loss curve is above -10 dB at around 60 GHz. As the distance increased, i.e., as the disc was moved slightly to the right, the impedance bandwidth decreased by almost 13 GHz, covering only the V and W bands (Figure 6(c)). Reduction of impedance bandwidth can also occur if we increase or decrease the size of the partial ground side "gl" (Figure 6(d)).

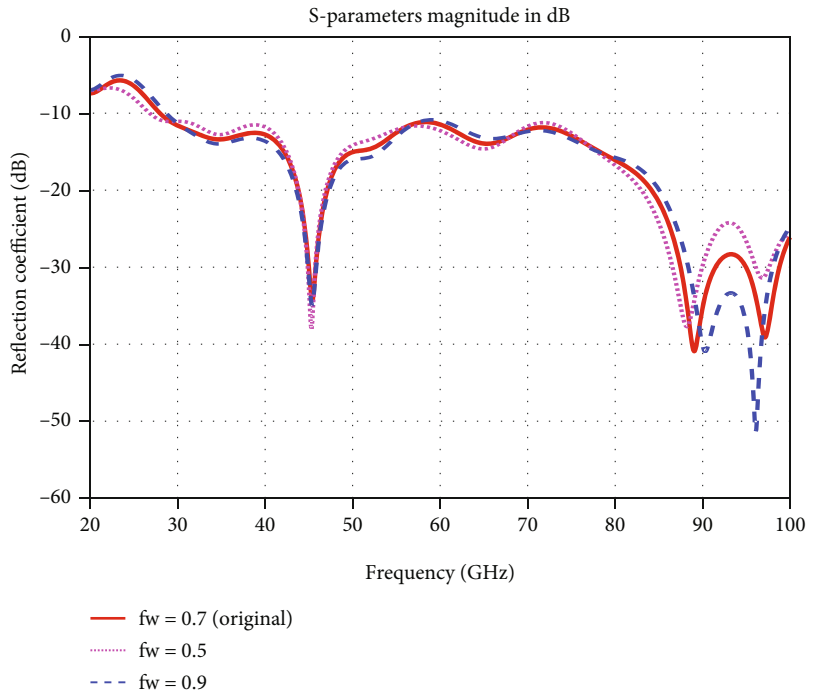

(a)

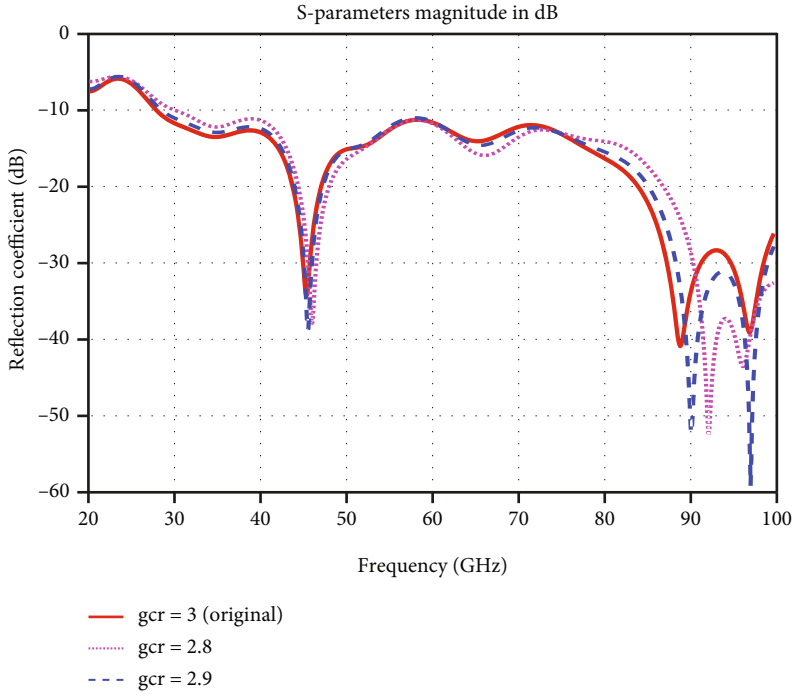

(b)

Figure 6: Continued.

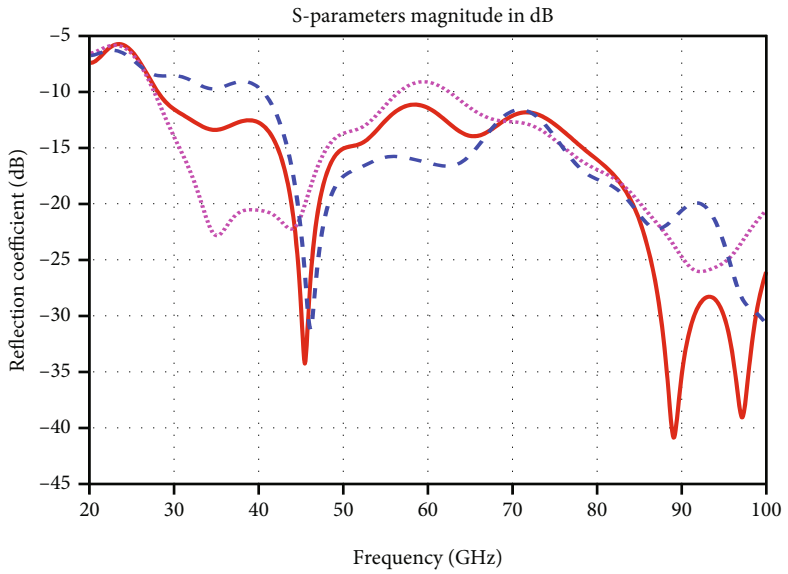

(c)

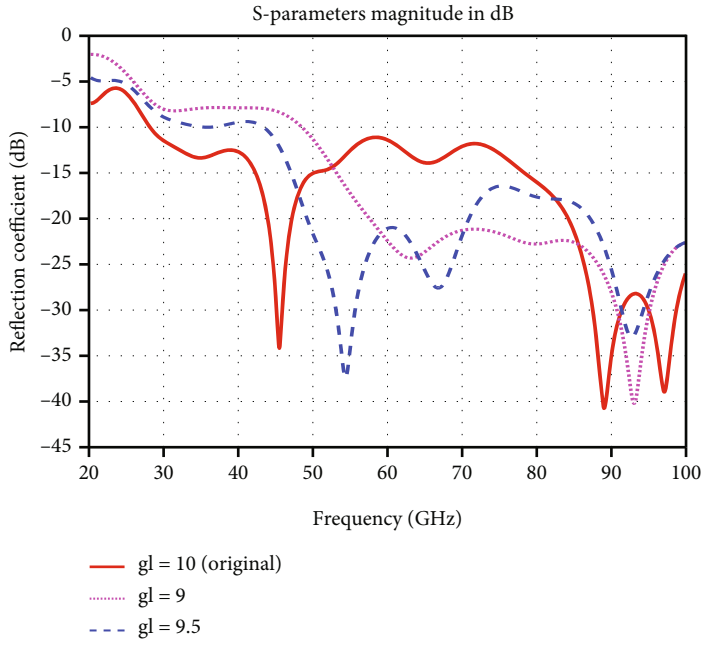

(d)

Figure 6: Changes in parameters have an impact on return loss: (a) feed width ("fw"), (b) ground circular slot radius ("gcr"), (c) disc position ("or"), and (d) partial ground length ("gl").

Table 2: Antenna parametric change results.

Parameters at 60 GHz	Final design	fw = 0.5 (mm)	fw = 0.9 (mm)	or = 1.8 (mm)	or = 2.2 (mm)	gcr = 2.8 (mm)	gcr = 2.9 (mm)	gl = 9 (mm)	gl = 9.5 (mm)
Return loss magnitude (dB)	-11.25	-12.06	-10.76	-8.91	-16.18	-11.40	-11.13	-22.49	-21.01
Gain (dBi)	5.704	5.529	5.858	5.989	4.999	5.634	5.674	6.322	6.425
Radiation efficiency (%)	89.06	88.59	89.35	88.71	88.69	89.76	89.65	92.29	87.89

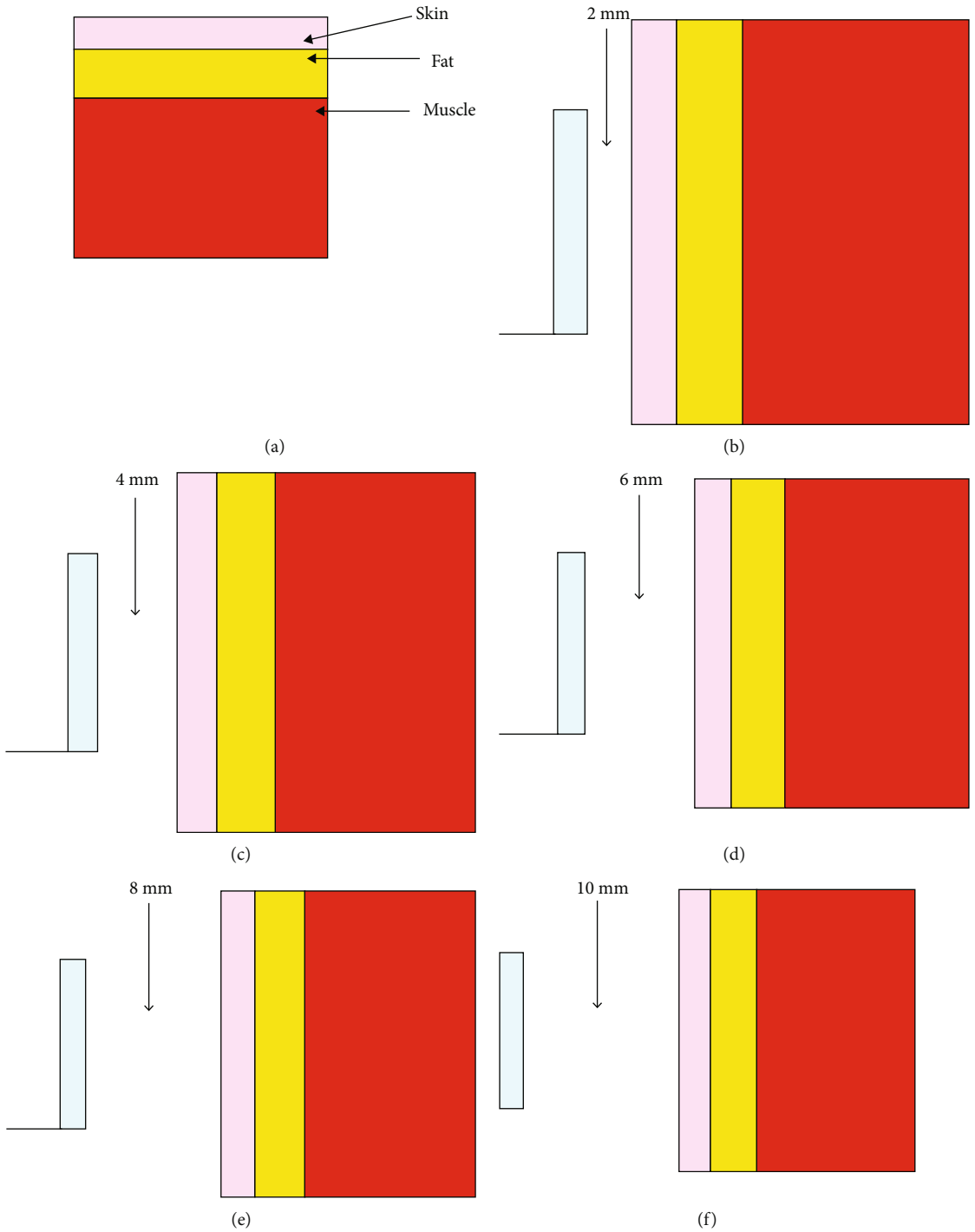

Figure 7: (a) Outermost layers of the phantom, antennas placed (b) 2 mm, (c) 4 mm, (d) 6 mm, (e) 8 mm, and (f) 10 mm away from the phantom.

Table 3: Dimension and physical properties of skin, fat, and muscle at 60 GHz [28].

Phantom layers	Dimension (mm)			Relative permittivity	Conductivity	Average penetration depth (mm)
	Length	Width	Thickness			
Skin	18	14	2	7.98	36.39	0.48
Fat	18	14	3	3.13	2.82	3.37
Muscle	18	14	10	12.86	52.83	0.41

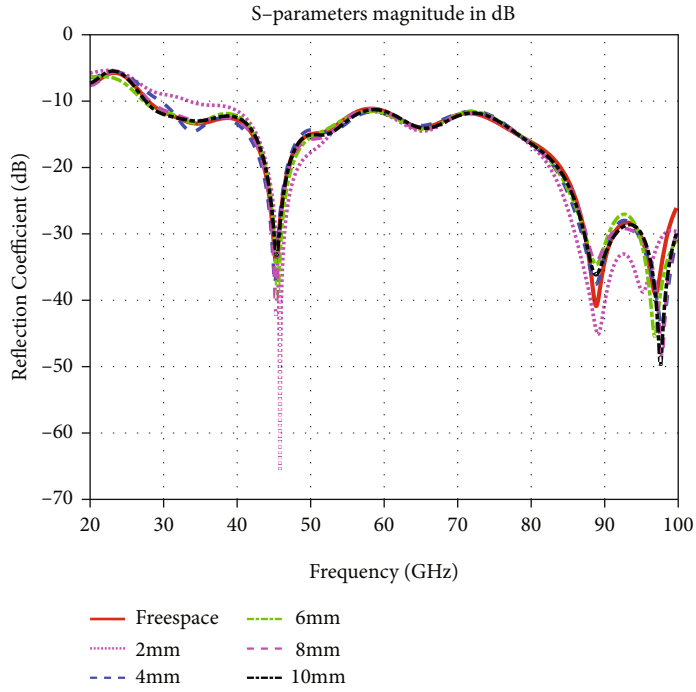

Figure 8: Simulations of on-body return loss at various distances.

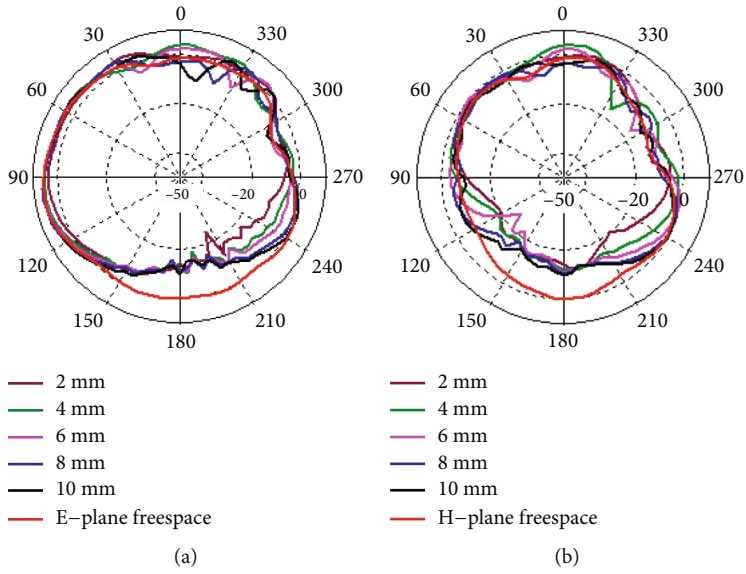

Figure 9: On-body radiation pattern at 60 GHz: (a) E plane and (b) H plane.

In general, at 60 GHz, the gain varied from 5 dBi to 6.4 dBi while the radiation efficiency ranged from 87.89% to 92.29% for various parametric changes. The detailed results for parametric changes are summarized in Table 2.

4. On-Body Simulation Results

Skin, fat, and muscle are the three outermost layers of the human body. The layers can be characterized by their relative permittivity or electric conductivity. These parameters vary at different frequencies, and for mmWave, these values are reported in [26]. Millimeter waves are easily blocked by obstacles, and at 60 GHz, on average, they can penetrate the skin up to a depth of 0.48 mm. For fat, this value is 3.37 mm, and for muscle, it is 0.41 mm. To mimic the human body, a phantom was created by stacking the three layers above each other (Figure 7(a)). Table 3 summarizes the physical characteristics of the phantom human. The space between the antenna and the human body model is shown in Figures 7(b)–7(f).

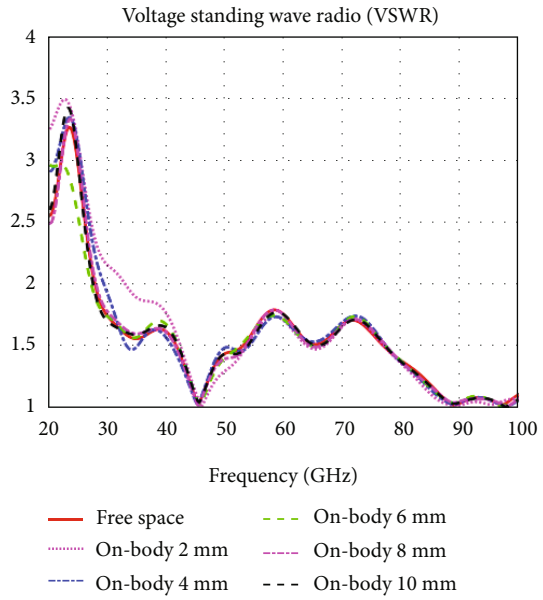

Figure 10: Free space and on-body (various distances) VSWR.

Table 4: On-body results at different gap distances.

Parameters at 60 GHz	Free space	On-body 2 mm	On-body 4 mm	On-body 6 mm	On-body 8 mm	On-body 10 m
Return loss	-11.25	-11.69	-11.64	-11.60	-11.29	-11.26
Gain (dBi)	5.704	6.137	5.806	5.813	6.046	5.922
Radiation efficiency (%)	89.06	67.48	75.79	79.02	81.95	83.71

Table 5: Free space comparison between different substrates.

Substrate	Relative permittivity	Thickness (mm)	Return loss magnitude (dB)	Gain (dBi)	Radiation efficiency (%)
100% polyester	1.9	1.5	-11.25	5.70	89.06
Jeans	1.7	1	-11.16	5.34	90.38
Denim	1.88	1.5	-11.20	5.83	89.04
Silk	1.75	1.16	-10.61	5.68	89.36
Tween	1.69	1.37	-11.38	6.32	88.71
Panama	2.12	1.04	-09.92	6.27	88.88
Felt	1.38	1.38	-13.15	6.76	91.69
Moleskin	1.45	1.17	-13.08	5.88	91.33
Cotton	1.63	1.5	-11.97	6.99	88.96
Quartzel fabric	1.95	1.5	-11.36	5.66	89.42
Cordura/lycra	1.5	0.5	-14.10	5.91	93.95

On-body simulations were carried out by placing the antenna at five different positions away from the phantom, starting at 2 mm (Figure 7(b)) and ending at 10 mm. When compared to open space, the antenna's impedance bandwidth reduced by almost 10 GHz when it was closest to the phantom. At this distance, the antenna is covering the V and W bands. As the gap between the antenna and the phantom increased, the return loss curves were almost identical. The resonant frequencies hardly shifted at these distances (Figure 8).

At close range, a grating radiation pattern can be seen in both the E and H planes. The radiation pattern becomes comparable to free space patterns as the gap distance increases. The E plane has some backward radiation towards the phantom at these distances (Figure 9(a)). The H plane does not exhibit any backward radiation for distances up to 4 mm (Figure 9(b)). The maximum gain at 60 GHz increased to a value of more than 6 dBi at a gap distance of 2 mm and 8 mm. Radiation efficiency at 2 mm decreased to 67.48% and gradually increased to 83.71% at the furthest

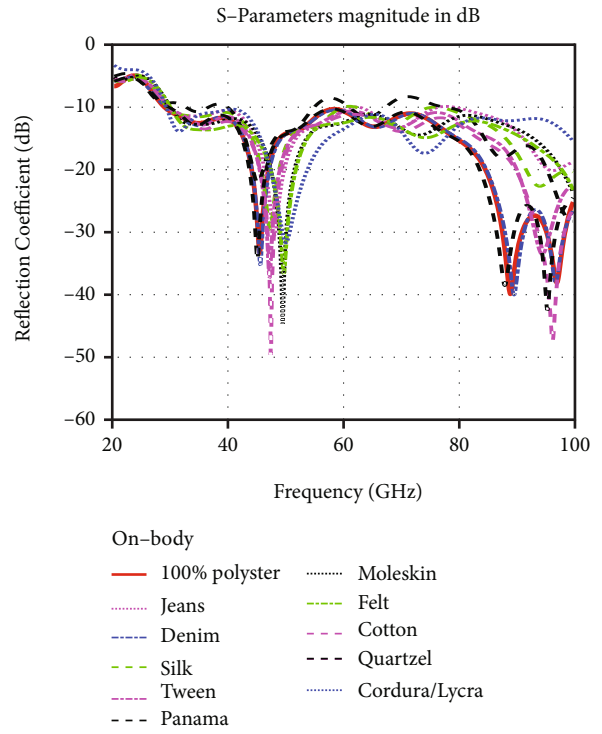

Figure 11: Simulated on-body return loss at different distances.

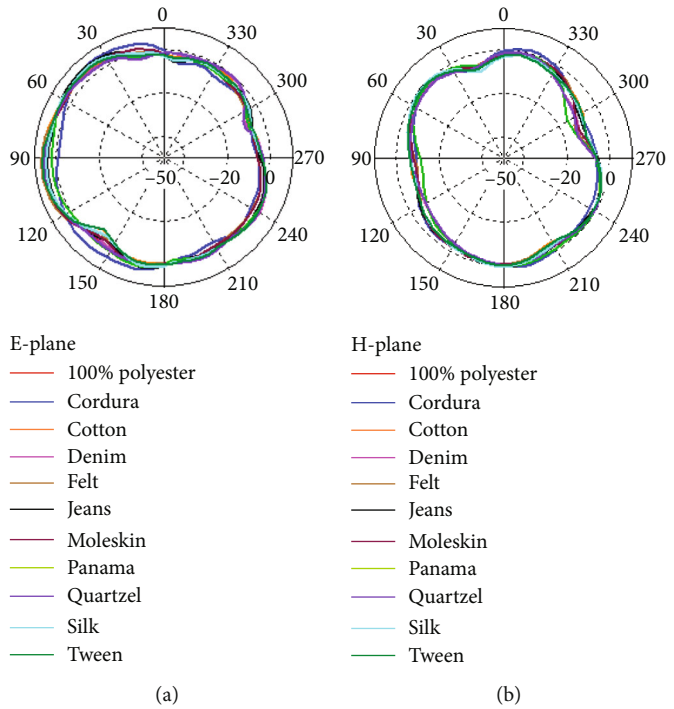

Figure 12: Comparison of several textile substrates' 60 GHz radiation patterns in free space: (a) E plane and (b) H plane.

distance, which is similar to free space efficiency. Figure 10 shows the free space and on-body VSWR for various distances away from the body. Results show that the distance between this antenna and the human phantom does affect significantly the VSWR. Results show that the distance between this antenna and the human phantom does affect the VSWR significantly. The on-body and free space simulated VSWR results are very close to each other over the large frequency range as shown in Figure 10. On-body simulation results are summarized in Table 4. Even though the

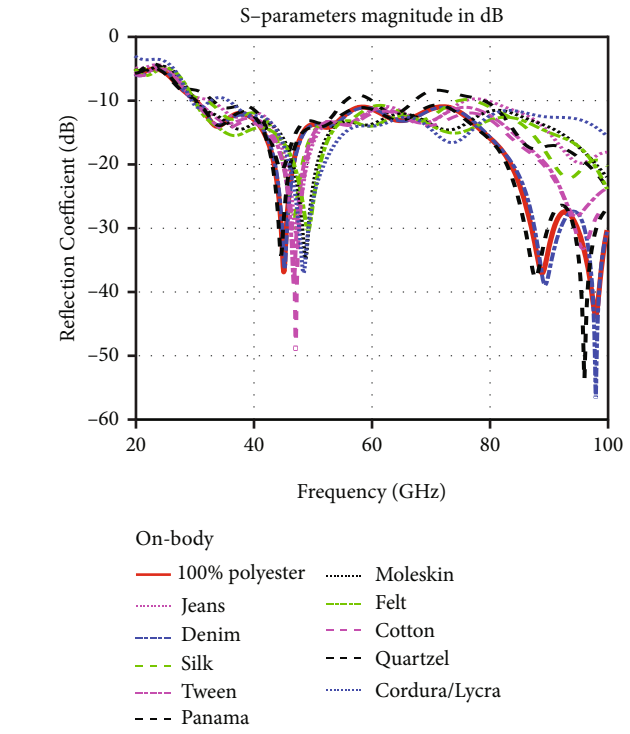

Figure 13: Different textile substrate on-body return losses.

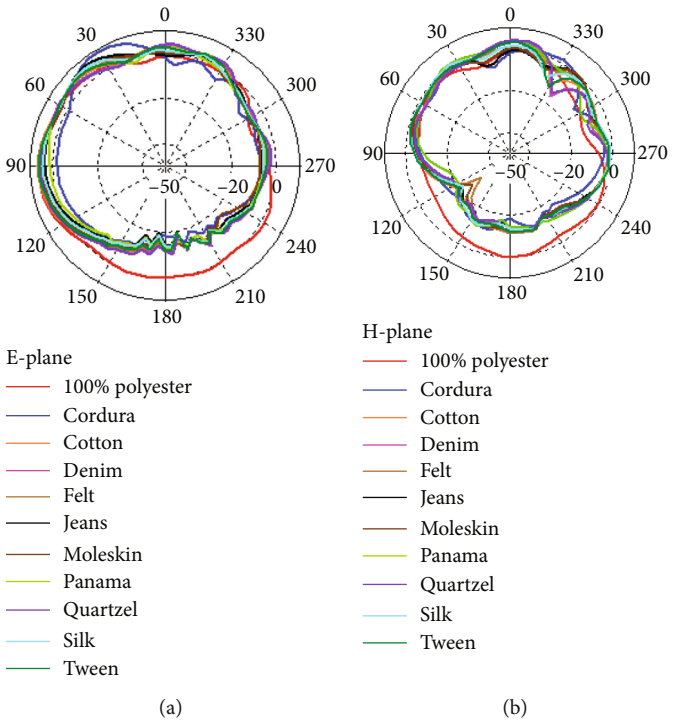

Figure 14: Comparison of on-body 60 GHz radiation patterns of different textile substrates: (a) E plane and (b) H plane.

Table 6: On-body comparison between different substrates.

Substrate	Relative permittivity	Thickness (mm)	Return loss magnitude (dB)	Gain (dBi)	Radiation efficiency (%)
100% polyester	1.9	1.5	-11.64	5.81	75.79
Jeans	1.7	1	-12.03	6.80	73.20
Denim	1.88	1.5	-11.57	5.79	75.73
Silk	1.75	1.16	-11.36	6.07	73.08
Tween	1.69	1.37	-11.96	5.99	74.06
Panama	2.12	1.04	-10.30	6.43	73.94
Felt	1.38	1.38	-14.41	6.25	75.44
Moleskin	1.45	1.17	-14.11	5.98	74.38
Cotton	1.63	1.5	-12.46	6.59	75.04
Quartzel fabric	1.95	1.5	-11.71	5.72	76.08
Cordura/lycra	1.5	0.5	-14.38	8.97	74.40

Table 7: Comparison with other articles.

Antenna	Size length (L) and width (W) mm	Operating frequency	Relative permittivity	Substrate material	Bandwidth (GHz) at -10 dB	Gain (dBi)	Efficiency (%)	Antenna type
Ref [15]	50 × 50	6.95-8.68 GHz	10	ECCOSTOCK HiK	6.95-8.68	5.00	*	DRA antenna
Ref [16]	*	3.89 GHz	10	ECCOSTOCKHIK	3.50-4.95	5.2	*	DRA MIMO
Ref [17]	350 × 350	3.23–3.59 GHz	10	ECCOSTOCK HiK	3.23–3.59	6.00	*	DRA antenna
This paper	10 × 7	60 GHz	1.9	Polyester substrate	Wideband	5.70	89.06	Single antenna

*Exact value not provided.

human body phantom is made of lossy material, the antenna performance is not much affected by it.

5. Various Textile Substrates

We analyzed the antenna's performance further by replacing the polyester substrate with ten different textile substrates. These substrates have different relative permittivity and thickness. Only the thicknesses of these substrates were modified, as they were the same as the polyester. The list of all ten textiles along with their detailed parameters and 60 GHz free space results is summarized in Table 5.

With the exception of the panama textile, the free space impedance bandwidth of nine other textile substrates is well matched to the polyester. The return loss curve of panama was above −10 dB at certain frequencies in the V_a and V bands (Figure 11). The 60 GHz radiation patterns of all ten substrates are very comparable to polyester in both the E and H planes (Figure 12). The radiation efficiency of all the ten substrates was very close to polyester. Tween and panama's efficiency was a bit lower than that of polyester's, while cordura/lycra's efficiency was highest at 93.95%. Cotton and felt's maximum gain at 60 GHz was almost 7 dBi, while the gain of the rest of the textiles was very similar to polyester's value.

The antenna was kept 2 mm away from the phantom for on-body placement. Each of the ten substrates was used to replace the polyester substrate, just like empty space. Like free space, the polyester substrate was replaced by each of the ten substrates. The impedance bandwidth is very close to that of free space (see Figure 13). Similar to the previous section's on-body results, the 60 GHz E plane radiation pattern for all ten substrates is grated (Figure 14(a)). The H plane has an insignificant amount of backward radiation (Figure 14(b)). No significant amount of change was seen on the maximum gain of these substrates when compared to free space. The radiation efficiency varied between 73 and 76%. See Table 6 for more details.

The proposed antenna is compared to other articles in Table 7. The proposed antennas in [1–17] work at lower frequency ranges, and the bandwidth and other performance parameters are good. However, the proposed antenna in this study works at a higher frequency band. This antenna shows very large bandwidth, and at -10 dB impedance, it shows 28 GHz to 100 GHz bandwidth. In addition, this proposed antenna has a different substrate material compared to the antennas presented in [15–17]. The physical size of the proposed antenna is also compact due to its high operating frequency.

6. Conclusion

In this paper, a superwideband QSC textile antenna design is presented. Due to a lack of proper facilities, no measurements were taken and we have only offered simulation results. Design and simulation were done using CST, which

is known for its reliability. The antenna's impedance bandwidth covered three different mmWave bands designated by IEEE. Due to high research interest in the 60 GHz V band, we have considered basing our study around the 60 GHz frequency. Even though the antenna was not resonant at this frequency, the antenna achieved high radiation efficiency and a satisfactory amount of gain. The impedance bandwidth is affected by the position of the radiating disc and the size of the ground edges, according to the parametric analysis. For on-body communications, the radiation patterns were distorted, especially close to the phantom.

The main design of the antenna was based on a nonconducting polyester textile substrate. For further evaluation, we replaced the substrate with ten different textiles. Both free space and on-body communication simulations were conducted. The results are very comparable to the polyester substrate. Good radiation efficiency and gain are maintained throughout the simulations. Compared to reported studies, this proposed design is unique in terms of operating bandwidth, radiation efficiency, and choice of materials. In the future, the upper frequency of the antenna can be further extended to investigate the performance of the antenna. Currently, the limitation is that we do not have the high computational resources to simulate the antenna for a wide range of frequencies, which requires more memory.

Data Availability

The data used to support the findings of this study are freely available at http://niremf.ifac.cnr.it/tissprop/.

Conflicts of Interest

The authors declare that they have no conflicts of interest to report regarding the present study.

Acknowledgments

The authors extend their appreciation to the Deanship of Scientific Research at King Khalid University for supporting this research through a Research Groups Program under Grant (RGP.1/49/42). The authors would like also to thank the support from the Taif University Researchers Supporting Project (TURSP-2020/26), Taif University, Taif, Saudi Arabia.

References

[1] J. F. Harvey, M. B. Steer, and T. S. Rappaport, "Exploiting high millimeter wave bands for military communications, applications, and design," *IEEE Access*, vol. 7, pp. 52350–52359, 2019.

[2] G. Chittimoju and U. D. Yalavarthi, "A comprehensive review on millimeter waves applications and antennas," *Journal of Physics: Conference Series*, vol. 1804, no. 1, article 012205, 2021.

[3] M. G. Sanchez, "Millimeter-wave communications," *Electronics*, vol. 9, no. 2, p. 251, 2020.

[4] B. Xu, R. Eike, A. Cliett, R. Cloud, and Y. Li, "A short review of textile applications in antenna design," *Trends in Textile Engineering & Fashion Technology*, vol. 1, no. 5, 2018.

[5] B. Almohammed, A. Ismail, and A. Sali, "Electro-textile wearable antennas in wireless body area networks: materials, antenna design, manufacturing techniques, and human body consideration—a review," *Textile Research Journal*, vol. 91, no. 5-6, pp. 646–663, 2021.

[6] X. Y. Wu, L. Akhoondzadeh-Asl, Z. P. Wang, and P. S. Hall, "Novel Yagi-Uda antennas for on-body communication at 60GHz," in *2010 Loughborough Antennas & Propagation Conference*, pp. 153–156, Loughborough, UK, 2010.

[7] S. Razafimahatratra, J. Sarrazin, A. Benlarbi-Delaï et al., "On-body propagation characterization with an H-plane substrate integrated waveguide (SIW) horn antenna at 60 GHz," in *2015 European Microwave Conference (EuMC)*, pp. 211–214, Paris, France, 2015.

[8] J. Puskely, M. Pokorny, J. Lacik, and Z. Raida, "Wearable disc-like antenna for body-centric communications at 61 GHz," *IEEE Antennas and Wireless Propagation Letters*, vol. 14, pp. 1490–1493, 2015.

[9] M. Ur-Rehman, N. A. Malik, X. Yang, Q. H. Abbasi, Z. Zhang, and N. Zhao, "A low profile antenna for millimeter-wave body-centric applications," *IEEE Transactions on Antennas and Propagation*, vol. 65, no. 12, pp. 6329–6337, 2017.

[10] N. Chahat, M. Zhadobov, L. Le Coq, S. I. Alekseev, and R. Sauleau, "Characterization of the interactions between a 60-GHz antenna and the human body in an off-body scenario," *IEEE Transactions on Antennas and Propagation*, vol. 60, no. 12, pp. 5958–5965, 2012.

[11] K. Islam, T. Hossain, and M. Khan, "A compact novel design of a 60 GHz antenna for body-centric communication," *International Journal on Communications Antenna and Propagation (IRECAP)*, vol. 10, no. 5, pp. 325–333, 2020.

[12] K. Islam, T. Hossain, M. M. Khan, M. Masud, and R. Alroobaea, "Comparative design and study of a 60 GHz antenna for body-centric wireless communications," *Computer Systems Science and Engineering*, vol. 37, no. 1, pp. 19–32, 2021.

[13] N. Chahat, M. Zhadobov, L. Le Coq, and R. Sauleau, "Wearable Endfire textile antenna for on-body communications at 60 GHz," *IEEE Antennas and Wireless Propagation Letters*, vol. 11, pp. 799–802, 2012.

[14] N. Chahat, M. Zhadobov, S. A. Muhammad, L. Le Coq, and R. Sauleau, "60-GHz textile antenna Array for body-centric communications," *IEEE Transactions on Antennas and Propagation*, vol. 61, no. 4, pp. 1816–1824, 2013.

[15] U. Illahi, J. Iqbal, M. I. Sulaiman et al., "Design of new circularly polarized wearable dielectric resonator antenna for off-body communication in WBAN applications," *IEEE Access*, vol. 7, pp. 150573–150582, 2019.

[16] J. Iqbal, U. Illahi, M. I. Sulaiman, M. M. Alam, M. M. Su'ud, and M. N. Yasin, "Mutual coupling reduction using hybrid technique in wideband circularly polarized MIMO antenna for WiMAX Applications," *Access*, vol. 7, pp. 40951–40958, 2019.

[17] J. Iqbal, U. Illahi, M. N. M. Yasin, M. A. Albreem, and M. F. Akbar, "Bandwidth enhancement by using parasitic patch on dielectric resonator antenna for sub-6 GHz 5G NR bands application," *Alexandria Engineering Journal*, vol. 61, no. 6, pp. 5021–5032, 2022.

[18] A. N. Khan, A. A. Ihalage, Y. Ma, B. Liu, Y. Liu, and Y. Hao, "Deep learning framework for subject-independent emotion detection using wireless signals," *PLoS One*, vol. 16, no. 2, article e0242946, 2021.

[19] A. Verner and D. Butvinik, "A machine learning approach to detecting sensor data modification intrusions in WBANs," in *2017 16th IEEE International Conference on Machine Learning and Applications (ICMLA)*, pp. 161–169, Cancun, Mexico, 2017.

[20] S. B. Roshni, M. P. Jayakrishnan, P. Mohanan, and K. P. Surendran, "Design and fabrication of an E-shaped wearable textile antenna on PVB-coated hydrophobic polyester fabric," *Smart Materials and Structures*, vol. 26, no. 10, article 105011, 2017.

[21] Y. Mukai and M. Suh, "Development of a conformal woven fabric antenna for wearable breast hyperthermia," *Fashion and Textiles*, vol. 8, no. 1, p. 7, 2021.

[22] J. G. Joshi and S. S. Pattnaik, "Polyester based wearable microstrip patch antenna," in *2013 IEEE Applied Electromagnetics Conference (AEMC)*, pp. 1-2, Bhubaneswar, India, 2013.

[23] K. Fujiwara, H. Shimasaki, and K. Morimoto, "Studies on a fabric feed line sewn to a flexible slot antenna," in *2016 International Workshop on Antenna Technology (iWAT)*, pp. 11–14, Cocoa Beach, FL, USA, 2016.

[24] P. J. Soh, G. A. E. Vandenbosch, X. Chen, P. S. Kildal, S. L. Ooi, and H. Aliakbarian, "Wearable textile antennas' efficiency characterization using a reverberation chamber," in *2011 IEEE International Symposium on Antennas and Propagation (APSURSI)*, pp. 810–813, Spokane, WA, USA, 2011.

[25] M. Wissem, EL, L. O. ImenSfar, and J.-M. Ribero, "A textile EBG-based antenna for future 5G-IoT millimeter-wave applications," *Electronics*, vol. 10, no. 2, p. 154, 2021.

[26] M. S. Alam, M. T. Islam, N. Misran, and J. S. Mandeep, "A wideband microstrip patch antenna for 60 GHz wireless applications," *Elektronica and Elektrotechniek*, vol. 19, no. 9, pp. 65–70, 2013.

[27] M. M. Khan, K. Islam, M. N. A. Shovon, M. Baz, and M. Masud, "Design of a novel 60 GHz millimeter wave Q-slot antenna for body-centric communications," *International Journal of Antennas and Propagation*, vol. 2021, Article ID 9795959, 12 pages, 2021.

[28] D. Andreuccetti, R. Fossi, and C. Petrucci, *Calculation of the Dielectric Properties of Body Tissues*, Italian National Research Council, IFAC-CNR, Florence, Italy, 2005.